Isoscalar single-pion production in the region of Roper and $d^*(2380)$ resonances

The WASA-at-COSY Collaboration

P. Adlarson [a,1], W. Augustyniak [b], W. Bardan [c], M. Bashkanov [d,*], F.S. Bergmann [e], M. Berłowski [f], H. Bhatt [g], A. Bondar [h,i], M. Büscher [j,2,3], H. Calén [a], I. Ciepał [k], H. Clement [l,m], E. Czerwiński [c], K. Demmich [e], R. Engels [j], A. Erven [n], W. Erven [n], W. Eyrich [o], P. Fedorets [j,p], K. Föhl [q], K. Fransson [a], F. Goldenbaum [j], A. Goswami [j,r], K. Grigoryev [j,s,4], C.-O. Gullström [a], L. Heijkenskjöld [a,1], V. Hejny [j], N. Hüsken [e], L. Jarczyk [c], T. Johansson [a], B. Kamys [c], G. Kemmerling [n,5], G. Khatri [c,6], A. Khoukaz [e], O. Khreptak [c], D.A. Kirillov [t], S. Kistryn [c], H. Kleines [n,5], B. Kłos [u], W. Krzemień [c], P. Kulessa [k], A. Kupść [a,f], A. Kuzmin [h,i], K. Lalwani [v], D. Lersch [j], B. Lorentz [j], A. Magiera [c], R. Maier [j,w], P. Marciniewski [a], B. Mariański [b], H.-P. Morsch [b], P. Moskal [c], H. Ohm [j], W. Parol [k], E. Perez del Rio [l,m,7], N.M. Piskunov [t], D. Prasuhn [j], D. Pszczel [a,f], K. Pysz [k], A. Pyszniak [a,c], J. Ritman [j,w,x], A. Roy [r], Z. Rudy [c], O. Rundel [c], S. Sawant [g,j], S. Schadmand [j], I. Schätti-Ozerianska [c], T. Sefzick [j], V. Serdyuk [j], B. Shwartz [h,i], K. Sitterberg [e], T. Skorodko [l,m,y], M. Skurzok [c], J. Smyrski [c], V. Sopov [p], R. Stassen [j], J. Stepaniak [f], E. Stephan [u], G. Sterzenbach [j], H. Stockhorst [j], H. Ströher [j,w], A. Szczurek [k], A. Trzciński [b], R. Varma [g], M. Wolke [a], A. Wrońska [c], P. Wüstner [n], A. Yamamoto [z], J. Zabierowski [aa], M.J. Zieliński [c], J. Złomańczuk [a], P. Żuprański [b], M. Żurek [j]

[a] Division of Nuclear Physics, Department of Physics and Astronomy, Uppsala University, Box 516, 75120 Uppsala, Sweden
[b] Department of Nuclear Physics, National Centre for Nuclear Research, ul. Hoza 69, 00-681, Warsaw, Poland
[c] Institute of Physics, Jagiellonian University, prof. Stanisława Łojasiewicza 11, 30-348 Kraków, Poland
[d] School of Physics and Astronomy, University of Edinburgh, James Clerk Maxwell Building, Peter Guthrie Tait Road, Edinburgh EH9 3FD, United Kingdom
[e] Institut für Kernphysik, Westfälische Wilhelms-Universität Münster, Wilhelm-Klemm-Str. 9, 48149 Münster, Germany
[f] High Energy Physics Department, National Centre for Nuclear Research, ul. Hoza 69, 00-681, Warsaw, Poland
[g] Department of Physics, Indian Institute of Technology Bombay, Powai, Mumbai-400076, Maharashtra, India
[h] Budker Institute of Nuclear Physics of SB RAS, 11 akademika Lavrentieva prospect, Novosibirsk, 630090, Russia
[i] Novosibirsk State University, 2 Pirogova Str., Novosibirsk, 630090, Russia
[j] Institut für Kernphysik, Forschungszentrum Jülich, 52425 Jülich, Germany
[k] The Henryk Niewodniczański Institute of Nuclear Physics, Polish Academy of Sciences, 152 Radzikowskiego St, 31-342 Kraków, Poland
[l] Physikalisches Institut, Eberhard-Karls-Universität Tübingen, Auf der Morgenstelle 14, 72076 Tübingen, Germany
[m] Kepler Center for Astro and Particle Physics, Eberhard Karls University Tübingen, Auf der Morgenstelle 14, 72076 Tübingen, Germany
[n] Zentralinstitut für Engineering, Elektronik und Analytik, Forschungszentrum Jülich, 52425 Jülich, Germany
[o] Physikalisches Institut, Friedrich-Alexander-Universität Erlangen–Nürnberg, Erwin-Rommel-Str. 1, 91058 Erlangen, Germany
[p] Institute for Theoretical and Experimental Physics, State Scientific Center of the Russian Federation, Bolshaya Cheremushkinskaya 25, 117218 Moscow, Russia
[q] II. Physikalisches Institut, Justus-Liebig-Universität Gießen, Heinrich-Buff-Ring 16, 35392 Giessen, Germany
[r] Department of Physics, Indian Institute of Technology Indore, Khandwa Road, Indore-452017, Madhya Pradesh, India

* Corresponding author.
 E-mail address: mikhail.bashkanov@ed.ac.uk (M. Bashkanov).
[1] Present address: Institut für Kernphysik, Johannes Gutenberg-Universität Mainz, Johann-Joachim-Becher Weg 45, 55128 Mainz, Germany.
[2] Present address: Peter Grünberg Institut, PGI-6 Elektronische Eigenschaften, Forschungszentrum Jülich, 52425 Jülich, Germany.
[3] Present address: Institut für Laser- und Plasmaphysik, Heinrich-Heine Universität Düsseldorf, Universitätsstr. 1, 40225 Düsseldorf, Germany.
[4] Present address: III. Physikalisches Institut B, Physikzentrum, RWTH Aachen, 52056 Aachen, Germany.
[5] Present address: Jülich Centre for Neutron Science JCNS, Forschungszentrum Jülich, 52425 Jülich, Germany.
[6] Present address: Department of Physics, Harvard University, 17 Oxford St., Cambridge, MA 02138, USA.
[7] Present address: INFN, Laboratori Nazionali di Frascati, Via E. Fermi, 40, 00044 Frascati (Roma), Italy.

[s] *High Energy Physics Division, Petersburg Nuclear Physics Institute, Orlova Rosha 2, Gatchina, Leningrad district 188300, Russia*
[t] *Veksler and Baldin Laboratory of High Energiy Physics, Joint Institute for Nuclear Physics, Joliot-Curie 6, 141980 Dubna, Moscow region, Russia*
[u] *August Chełkowski Institute of Physics, University of Silesia, Uniwersytecka 4, 40-007, Katowice, Poland*
[v] *Department of Physics, Malaviya National Institute of Technology Jaipur, 302017, Rajasthan, India*
[w] *JARA-FAME, Jülich Aachen Research Alliance, Forschungszentrum Jülich, 52425 Jülich, and RWTH Aachen, 52056 Aachen, Germany*
[x] *Institut für Experimentalphysik I, Ruhr-Universität Bochum, Universitätsstr. 150, 44780 Bochum, Germany*
[y] *Department of Physics, Tomsk State University, 36 Lenina Avenue, Tomsk, 634050, Russia*
[z] *High Energy Accelerator Research Organisation KEK, Tsukuba, Ibaraki 305-0801, Japan*
[aa] *Department of Astrophysics, National Centre for Nuclear Research, Box 447, 90-950 Łódź, Poland*
[ab] *Helmholtz-Institut für Strahlen- und Kernphysik, Rheinische Friedrich-Wilhelms-Universität Bonn, Nußallee 14–16, 53115 Bonn, Germany*

A R T I C L E   I N F O

A B S T R A C T

Exclusive measurements of the quasi-free $pn \to pp\pi^-$ and $pp \to pp\pi^0$ reactions have been performed by means of pd collisions at $T_p = 1.2$ GeV using the WASA detector setup at COSY. Total and differential cross sections have been obtained covering the energy region $T_p = 0.95$–1.3 GeV ($\sqrt{s} = 2.3$–2.46 GeV), which includes the regions of $\Delta(1232)$, $N^*(1440)$ and $d^*(2380)$ resonance excitations. From these measurements the isoscalar single-pion production has been extracted, for which data existed so far only below $T_p = 1$ GeV. We observe a substantial increase of this cross section around 1 GeV, which can be related to the Roper resonance $N^*(1440)$, the strength of which shows up isolated from the Δ resonance in the isoscalar $(N\pi)_{I=0}$ invariant-mass spectrum. No evidence for a decay of the dibaryon resonance $d^*(2380)$ into the isoscalar $(NN\pi)_{I=0}$ channel is found. An upper limit of 180 μb (90% C.L.) corresponding to a branching ratio of 9% has been deduced.

1. Introduction

Single-pion production in nucleon–nucleon (NN) collisions may be separated into isoscalar and isovector production. Excitation of the $\Delta(1232)$ resonance and of higher-lying Δ states in the course of the collision process can only happen in an isovector process. Hence these are absent in isoscalar single-pion production, which comprises only isoscalar processes like the excitation of the Roper resonance $N^*(1440)$ and higher-lying N^* resonances – but also to the excitation and decay of the recently observed dibaryon state $d^*(2380)$ with $I(J^P) = 0(3^+)$ [1–4]. Both these resonances are the primary aim of this Letter.

At incident energies below 1 GeV, single-pion production is strongly characterized by excitation and decay of the $\Delta(1232)$ resonance. There have been several attempts in the past to extract the isoscalar production cross section [5–10], in order to reveal production processes other than the dominating Δ process. Since single-pion production in NN collisions is either purely isovector or isospin-mixed, the isoscalar cross section has to be obtained by combination of various cross section measurements. Most often the relation [5,6]:

$$\sigma_{NN \to NN\pi}(I=0) = 3(2\sigma_{np \to pp\pi^-} - \sigma_{pp \to pp\pi^0}) \qquad (1)$$

is used. Since here the difference of two usually big values enters, the experimental uncertainties appear generally large relative to the obtained absolute values. Previous experimental studies from near threshold up to 1 GeV incident energy give a large scatter of values with a tendency of being close to zero at low energies and increasing to values in the range of 1–2 mb [7–10] towards 1 GeV, in Ref. [5] even up to 4 mb.

In Ref. [10] the isoscalar cross sections have not been derived by use of eq. (1). Instead of using total cross sections a partial-wave analysis was applied to (unnormalized) angular and invariant mass distributions. The isoscalar cross section was then extracted from the observed asymmetries in the pion angular distribution – assuming that they exclusively derive from the interference of the isovector amplitudes with the isoscalar ones.

Here we report on first measurements of the isoscalar cross section from $T_p = 0.95$ GeV up to 1.3 GeV ($\sqrt{s} = 2.3$–2.46 GeV) by use of eq. (1). Aside from the $\Delta(1232)$ and $N^*(1440)$ excitations, this energy range covers the region of the $d^*(2380)$ dibaryon resonance. Whereas this resonance is considered to decay via an intermediate $\Delta\Delta$ system in general [11], Kukulin and Platonova [12] recently proposed an alternative scenario, where this resonance decays into the ΔN threshold state D_{12} with $I(J^P) = 1(2^+)$ by emission of a pion in relative p wave. Kinematically such a decay is hard to distinguish from that via an intermediate $\Delta\Delta$ system. However, contrary to the latter the decay via D_{12} causes a decay branch $d^*(2380) \to (NN\pi)_{I=0}$ because of the decay $D_{12} \to NN$. According to the SAID partial-wave analyses [13,14], the latter decay branch is 16–18%. Using a total d^* production cross section of about 1.7 mb for the observed decays into NN and $NN\pi\pi$ channels [11], we thus expect a peak cross section of about 350 μb for the route $pn \to d^*(2380) \to D_{12}\pi \to (NN\pi)_{I=0}$.

Following a suggestion of Bugg [15], $d^*(2380)$ could represent as well a $N^*(1440)N$ system. Such a scenario would cause, too, a decay of $d^*(2380)$ into the isoscalar $NN\pi$ system. Since the Roper resonance decays into the $N\pi$ channel with a probability of 55–75% [16], we expect in this case a cross section as large as 1.1–1.4 mb for the route $pn \to d^*(2380) \to N^*(1440)N \to (NN\pi)_{I=0}$.

2. Experiment

In order to utilize eq. (1) for the extraction of the isoscalar single-pion production, we have measured both reactions $pp \to pp\pi^0$ and $pn \to pp\pi^-$ simultaneously by use of their quasi-free processes in pd collisions. The experiment has been carried out at COSY (Forschungszentrum Jülich) at the WASA detector setup by using a proton beam with an energy of $T_p = 1.2$ GeV impinging on a deuterium pellet target [17,18]. By exploiting the Fermi momentum of the nucleons within the deuteron in the quasi-free scattering processes $pd \to pp\pi^0 + n_{spectator}$ and $pd \to pp\pi^- + p_{spectator}$, we cover the energy region $\sqrt{s} = 2.30$–2.44 GeV (corresponding to effective incident lab energies of $T_{lab} = 0.95$–1.3 GeV). This includes the regions of $\Delta(1232)$, $N^*(1440)$ and $d^*(2380)$ resonance excitations.

The hardware trigger utilized in this analysis required at least one charged hit in the forward detector as well as two recorded clusters in the central detector.

The quasi-free reaction $pd \to pp\pi^0 + n_{spectator}$ has been selected in the offline analysis by requiring one proton track in each of the forward and central detectors as well as two photon hits in the central detector, which can be traced back to the decay of a π^0 particle. The quasi-free reaction $pd \to pp\pi^- + p_{spectator}$ has been selected in the same way with the difference that now instead of two photon hits a π^- track has been required in the central detector. That way, the non-measured spectator four-momentum could be reconstructed by a kinematic fit with two and one over-constraints, respectively, which derive from the conditions for energy and momentum conservation and the π^0 mass. The achieved resolution in $\sqrt{s}$ was about 20 MeV.

The charged particles registered in the segmented forward detector of WASA have been identified by use of the $\Delta E - E$ energy loss method. For its application in the data analysis, all combinations of signals stemming from the five layers of the forward range hodoscope have been used. The charged particles in the central detector have been identified by their curved track in the magnetic field as well as by their energy loss in the surrounding plastic scintillator barrel and electromagnetic calorimeter.

Fig. 1 shows two sample spectra to demonstrate the quality of the events selected for the subsequent kinematic fits. On the top panel the $pp\gamma\gamma$-missing mass $MM_{pp\gamma\gamma}$ is plotted versus the $\gamma\gamma$-invariant mass $M_{\gamma\gamma}$ as observed in the quasi-free $pd \to pp\pi^0 + n_{spectator}$ reaction. The black circle denotes the applied cut. The π^0 reconstruction efficiency is 87% for the case that per event 1 proton in the forward detector as well as 1 proton and 2 neutrals in the central detector have been identified. On the bottom panel the momentum P of charged particles measured with the minidrift chamber within the solenoid is plotted versus the particle energy deposited in the plastic scintillator barrel for the quasi-free $pd \to pp\pi^- + p_{spectator}$ reaction. Negative momenta denote negatively charged particles, positive momenta correspondingly positively charged ones. Negative pions, positive pions and protons appear clearly separated. The black line shows the applied cut for the protons. The positive pions originate from the quasi-free two-pion production $pd \to np\pi^+\pi^- + p_{spectator}$. Their leakage into the proton band causes a contamination of the $pd \to pp\pi^- + p_{spectator}$ reaction of less than 1%.

In total, a sample of about 1006800 $pp\pi^0$ and 235000 $pp\pi^-$ events meeting all selection criteria has been obtained. The requirement that the two protons have to be each in the angular range covered by the forward and central detector and that the π^- and the gammas resulting from π^0 decay have to be in the angular range of the central detector reduces the overall acceptance to about 38% and 41%, respectively. The total reconstruction efficiency including all cuts and kinematical fitting has been 3.0% and 0.81%, respectively. The small efficiencies are due to the fact that we use only events, which have exactly three tracks in case of $pp\pi^-$ and four tracks in case of $pp\pi^0$, i.e., we discard events, which contain beam related background like bremsstrahlung gammas. In addition we require the tracks to give no hint for secondaries due to hadronic interactions in the detector material. This is particularly restrictive for tracks in the forward detector due to high-energy protons.

In order to understand the small total efficiencies, we illustrate the reduction of data events by the various steps of the offline data analysis for the case of the $pp\pi^-$ channel. In a first step all events, which meet the trigger condition for the $pp \to pp\pi^-$ reaction, are requested to represent charged tracks, a single one in the forward detector and two charged tracks in the central detector. In the next step we require by use of the MDC information
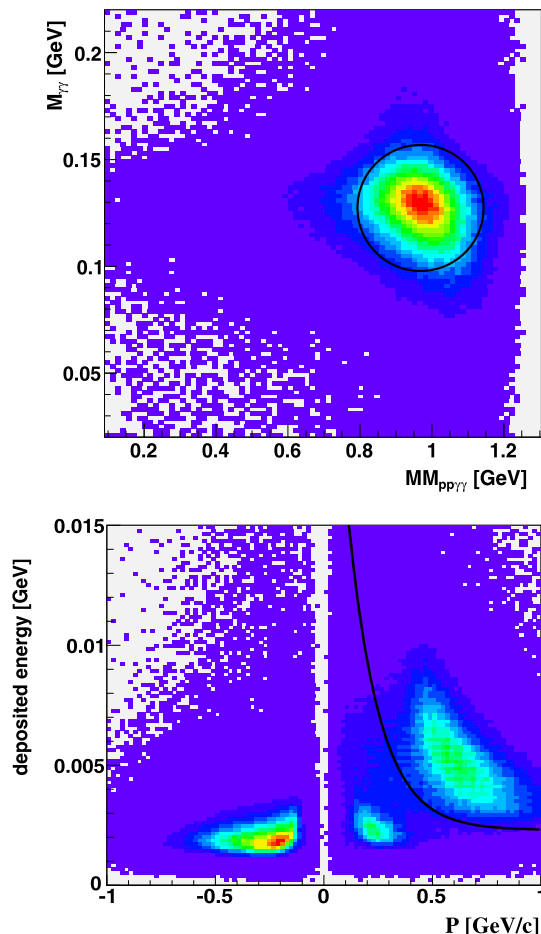

Fig. 1. (Color online.) Top: Plot of the $pp\gamma\gamma$-missing mass $MM_{pp\gamma\gamma}$ versus the $\gamma\gamma$-invariant mass $M_{\gamma\gamma}$ as observed in the quasi-free $pd \to pp\pi^0 + n_{spectator}$ reaction. The black circle denotes the applied cut. Bottom: Plot of the momentum P of charged particles measured with the minidrift chamber within the solenoid versus the particle energy deposited in the plastic scintillator barrel for the quasi-free $pd \to pp\pi^- + p_{spectator}$ reaction. Negative momenta denote negatively charged particles, positive momenta correspondingly positively charged ones.

that one of the two tracks in the central detector is of positive charge, whereas the other one is of negative charge. This reduces the candidate events by a factor of four. The third step requires the three charged tracks to be uniquely identified as two protons and one π^- particle due to their specific energy losses in the detector set-up without exhibiting any hadronic interaction with the detector material. As a consequence the candidate sample is reduced by a factor of six. The fourth step checks kinematical conditions for emission angles and missing masses. It removes events with corrupted kinematic information and leads to another factor of four reduction in the candidate events. Finally in the last step the kinematic fit is applied, which gives another 20% reduction.

We note that the inefficiencies of the various detector elements were studied in rare decays studies, where e.g. in the measurement of Dalitz plot asymmetries a 4–5 digits precision was required [19].

In order to check the reliability of our data analysis, comprehensive MC simulations of reactions and detector set-up have been performed using a cocktail of 16 reaction channels, which comprise elastic scattering, single-pion and double-pion production. That way a realistic scenario was generated, of how the reactions of interest were embedded in the cocktail of background reactions. These MC simulations reproduce the event reduction in the data by the various analysis steps on the percent level and show that the enrichment of proper events for the desired reaction channel

by the five analysis steps reaches 99% and better. *I.e.*, the contamination of the final sample due to background reactions is at most 1%.

Efficiency and acceptance corrections of the data have been performed by MC simulations of reaction process and detector setup. Since the data show substantial deviations from pure phase-space distributions (see next chapter), the reaction process had to be modeled with Δ and *Roper* excitations, in order to achieve agreement between data and MC simulation and thus a consistent procedure for the data reduction process. The MC simulations based on pure phase-space and model descriptions will be discussed in the next chapter.

Since WASA does not cover the full reaction phase space, albeit a large fraction of it, these corrections are not fully model independent. The hatched gray histograms in Figs. 3–6 give an estimate for these systematic uncertainties. As a measure of these we have taken the difference between model corrected results and those obtained by assuming simply pure phase space for the acceptance corrections. Though this very conservative estimate considerably exaggerates the systematic uncertainties, since ignoring even the well-known dominating Δ excitation is not physically meaningful, it nevertheless demonstrates the stability of the corrections. Compared to the uncertainties in these corrections, systematic errors associated with modeling the reconstruction of particles are negligible.

The absolute normalization of the data has been obtained by comparison of the quasi-free single pion production process $pd \rightarrow pp\pi^0 + n_{spectator}$ to previous bubble-chamber results for the total cross section of the $pp \rightarrow pp\pi^0$ reaction [20–22]. That way, the uncertainty in the absolute normalization of our data is essentially that of the previous $pp \rightarrow pp\pi^0$ data, *i.e.* in the order of 5–15%. For the $pn \rightarrow pp\pi^-$ reaction the extrapolation to full phase space introduces some model dependence, which gives an uncertainty in the order of 5% in the absolute scale of this cross section relative to the one of the $pp \rightarrow pp\pi^0$ reaction.

In order to have some measure of systematic uncertainties in the data reduction process, we varied the conditions for cuts and fits within reasonable boundaries both in data analyses and MC simulations. As a result we obtained a maximum of 7% change in the deduced $pn \rightarrow pp\pi^-$ cross section relative to the one for the $pp \rightarrow pp\pi^0$ channel.

Together with the one for the acceptance correction we end up with a systematic error of 8% for the $pp \rightarrow pp\pi^-$ cross section relative to the one of the $pp \rightarrow pp\pi^0$ reaction.

3. Results and discussion

In order to determine the energy dependence of the total cross sections for the $pp \rightarrow pp\pi^0$ and $pn \rightarrow pp\pi^-$ reactions, we have divided our data sample into bins of 50 MeV width in the incident energy T_p. The resulting total cross sections for these channels as well as for the isoscalar channel determined by use of eq. (1) are shown in Fig. 2 together with results from earlier measurements [5–10,20–31]. Our data for the $pp\pi^0$ channel exhibit a flat energy dependence in good agreement with previous data. For the $pp\pi^-$ channel our data show a slope slightly declining with increasing energy – also in agreement with previous results, which exhibit some scatter.

The isoscalar cross section as obtained by use of eq. (1) is displayed at the bottom panel of Fig. 2. Our data exhibit cross sections in the range of 2–5 mb. In the overlap region with previous results, at incident energies around 1 GeV, our data agree with those obtained by Dakhno et al. [5], but are higher than the results of Refs. [7,9,10]. The latter used cross sections for the $pp \rightarrow pp\pi^0$ reaction, which are higher by roughly 10% than those used in Ref. [5].
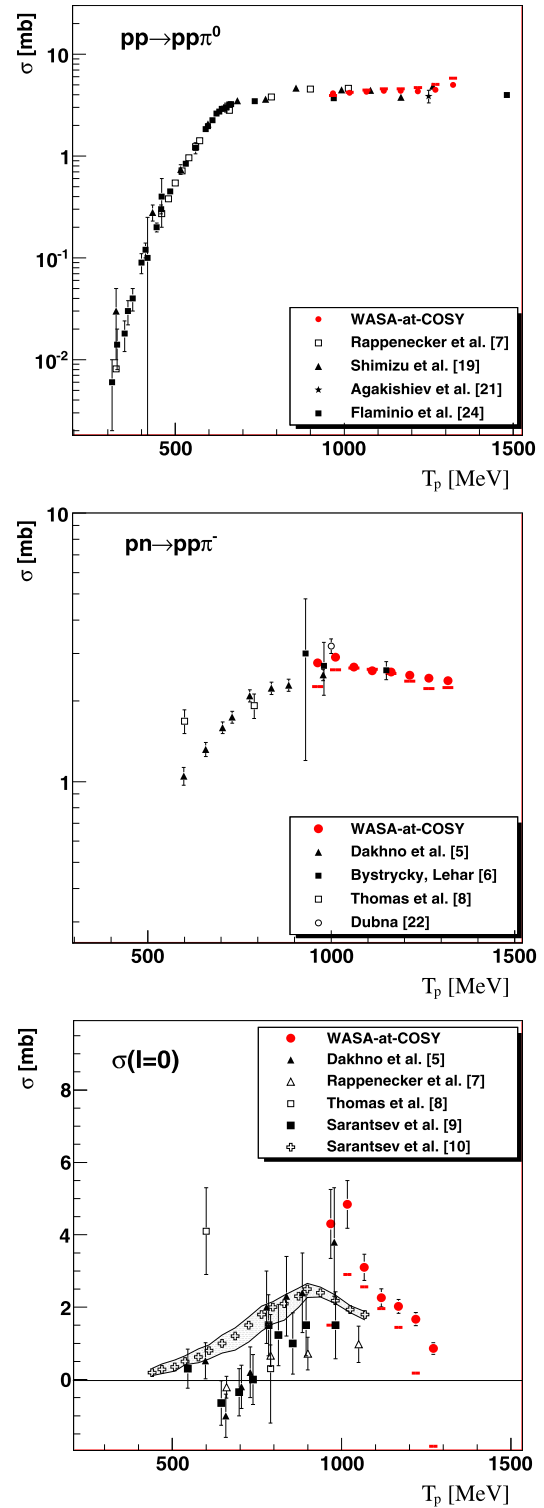
Fig. 2. (Color online.) Total cross sections in dependence of the incident proton energy T_p for the reactions $pp \rightarrow pp\pi^0$ (top), $pn \rightarrow pp\pi^-$ (middle) and the extracted isoscalar single-pion production cross section $\sigma(I=0)$ (bottom). Red solid circles denote the results of this work. The red horizontal bars represent the same data by use of a pure phase-space correction and serve just as an indication for the stability of the results under extreme assumptions. Other symbols give results from earlier work [5–10,20–31].

Also, in contrast to our experiment, where we measured both reactions simultaneously with the same detector setup – reducing thus systematic errors –, the previous results obtained at lower
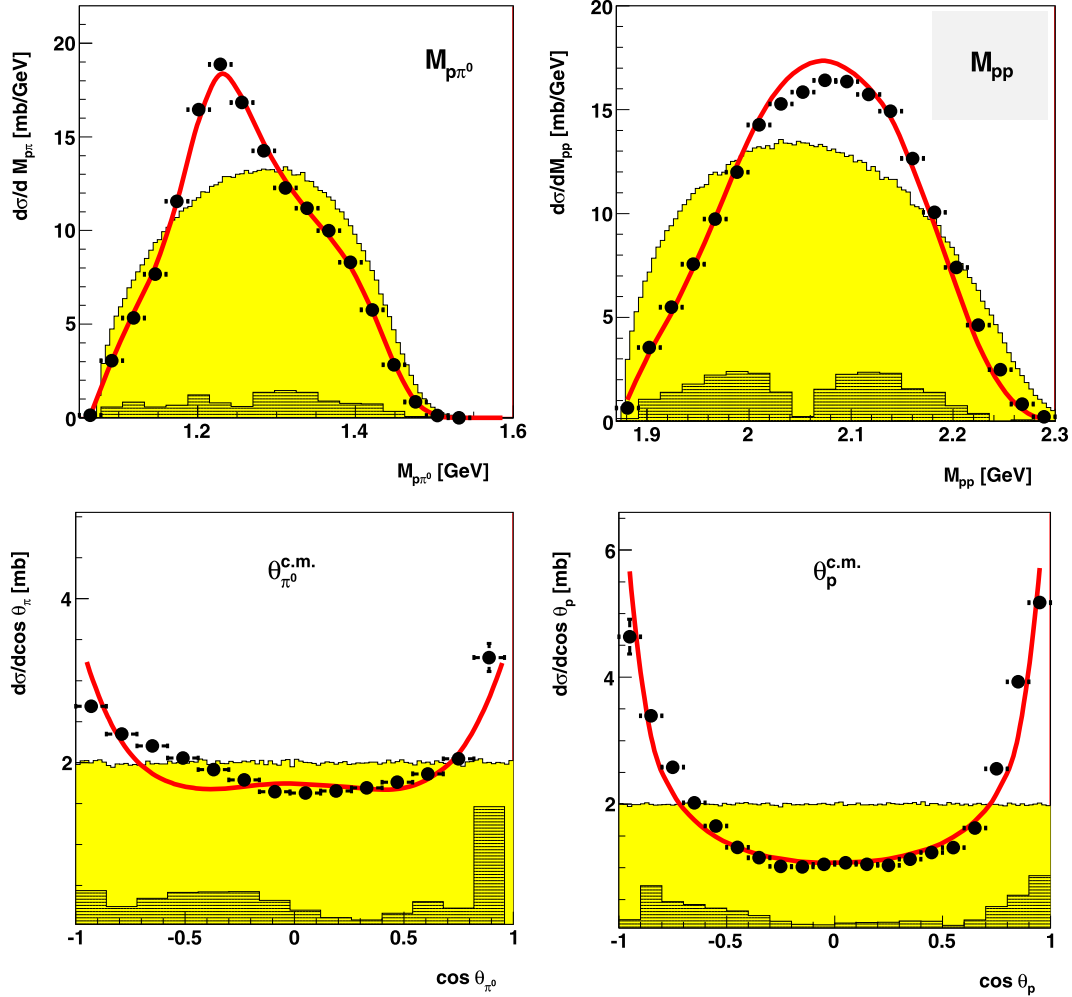
Fig. 3. (Color online.) Differential distributions of the $pp \rightarrow pp\pi^0$ reaction at $T_p = 1.2$ GeV for invariant-masses $M_{p\pi^0}$ (top left) and M_{pp} (top right) of $p\pi^0$ and pp subsystems, respectively, as well as for the c.m. angles of neutral pions $\Theta_{\pi^0}^{c.m.}$ (bottom left) and protons $\Theta_p^{c.m.}$ (bottom right). The hatched histograms indicate systematic uncertainties due to the restricted phase-space coverage of the data. The light-shaded (yellow) areas represent pure phase-space distributions, the solid lines are calculations of $\Delta(1232)$ and $N^*(1440)$ excitations by t-channel meson exchange – normalized in area to the data.

energies were obtained by use of independent measurements for $pp\pi^0$ and $pp\pi^-$ channels carried out under different conditions, partially using even interpolations for the cross section values. It is therefore not unlikely that all those shortcomings contribute to the large scatter of extracted values in the low-energy region.

By use of eq. (1) the 8% uncertainty in the absolute scale of our cross sections for the $pp\pi^-$ channel relative to those of the $pp\pi^0$ channel translates to an uncertainty of 30%, *i.e.* about 1.5 mb, in the absolute scale of the isoscalar cross section. Hence the discrepancy to the results of Ref. [10] may possibly not be as big as Fig. 2, bottom, seems to illustrate.

The results of Ref. [10] agree with those of Dakhno et al. [5] for $T_p < 0.9$ GeV. Only above there are discrepancies. Whereas the data point from Dakhno et al. at $T_p = 0.978$ GeV signals a further increase of the isoscalar cross section, the cross section deduced in Ref. [10] starts to decrease again at higher energies. This behavior appears to be very strange, since the Roper excitation – as the only isoscalar resonance process at low energies – keeps rising in strength up to 1 GeV beam energy and leveling off beyond, as we know from the analysis of two-pion production data [32,33]. The observed energy dependence of the isoscalar single-pion production given by the data from Dakhno et al. [5] and WASA is at least qualitatively close to that deduced for the Roper excitation in two-pion production.

When binned into $\sqrt{s}$ bins of 20 MeV, the differential distributions do not exhibit any particular energy dependence in their shapes – which is of no surprise, since the energy region covered in this measurement is dominated by Δ and Roper excitations with very smooth energy dependencies due to their large decay widths. Hence we refrain from showing all differential distributions for single $\sqrt{s}$ bins. We rather show them un-binned, *i.e.*, averaged over the full energy range of the measurement, which has the advantage of better statistics and less systematic uncertainties due to potential binning artifacts. Only for the $p\pi$-invariant mass distributions we show some energy bins as an example.

For a three-body final state there are four independent differential observables. We choose to show in this paper the differential distributions for the center-of-mass (c.m.) angles for protons and pions denoted by $\Theta_p^{c.m.}$ and $\Theta_{\pi^0}^{c.m.}$, respectively, as well as for the invariant masses $M_{p\pi}$ and M_{pp}. These distributions are shown in Figs. 3–4. The resolution in the angular distributions is 0.5–1°, the one in the invariant mass spectra 15–20 MeV.

All measured differential distributions are markedly different in shape from pure phase-space distributions (shaded areas in Figs. 3–6). They are reasonably well reproduced by model calculations for t-channel pion exchange leading to excitation and decay of $\Delta(1232)$ and $N^*(1440)$. This has been accomplished by utiliz-
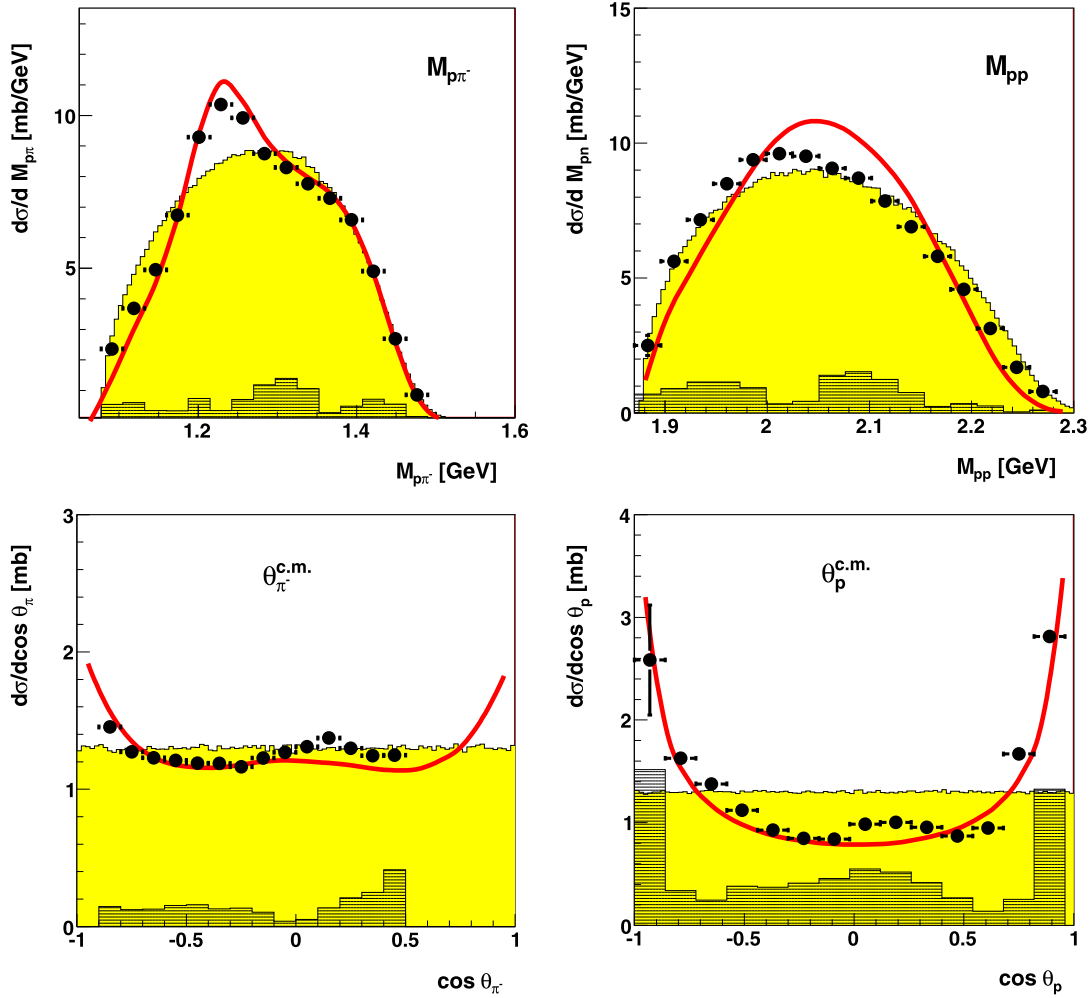
Fig. 4. (Color online.) The same as Fig. 3, but for the $pn \to pp\pi^-$ reaction.

ing the Valencia code for pion production [34]. The calculations are adjusted in area to the data in Figs. 3–6.

The proton angular distribution is strongly forward–backward peaked in both channels as expected for a peripheral reaction process. The pion angular distribution of the purely isovector $pp\pi^0$ channel, where the Δ excitation dominates, behaves as expected from the p-wave decay of the Δ resonance. For the isospin-mixed $pp\pi^-$ channel, where the Roper resonance contributes with a flat pion angular dependence, the observed pion angular distribution is less curved due the combined contributions from Δ and Roper decays. The observed asymmetries in the angular distributions are within the systematic errors.

The invariant mass spectra for $M_{p\pi^0}$ and $M_{p\pi^-}$ are both characterized by the Δ peak – though in the $M_{p\pi^0}$ spectrum much more pronounced than in the $M_{p\pi^-}$ spectrum. At the high-mass shoulder of the Δ peak the Roper excitation gets visible – in particular now in the $M_{p\pi^-}$ spectrum. As an example for the smooth energy dependence observed in the energy interval of interest here, we plot the $M_{p\pi^0}$ and $M_{p\pi^-}$ spectra for three energy bins in Fig. 5.

By application of eq. (1) to the invariant mass spectra, we obtain the isoscalar $p\pi$ invariant mass distribution, in which the isovector Δ process has to be absent. Fig. 6 exhibits the isoscalar $M_{p\pi}^{I=0}$ distribution, where indeed the Δ peak has vanished. The remaining structure at higher energies has to be attributed to the isoscalar Roper excitation (solid line). To our knowledge this is the

first time that the isoscalar Roper excitation could be visibly isolated in an invariant mass distribution.

The energy dependence of the total isoscalar cross section is displayed in Fig. 7 in dependence of the c.m. energy $\sqrt{s}$. The only apparent structure is an enhancement at $\sqrt{s} = 2.33$ GeV. However, its statistical significance is less than 3σ and hence not of statistical relevance.

At the location of the $d^*(2380)$ resonance the cross section exhibits no particular structure. In principle the resonance can interfere with the background, which is dominated by the Roper excitation. Since we are here just in the region of the nominal $N^*(1440)N$ threshold, this system is most likely in relative S wave yielding total angular momenta of 0 and 1. In order to interfere with the $d^*(2380)$ resonance, the $N^*(1440)N$ system would need to have a total angular momentum of 3, *i.e.*, would need to be in relative D wave – which is extremely unlikely at threshold. These considerations are also supported by the partial-wave decomposition given in Ref. [10] for the $np \to pp\pi^-$ reaction at $T_p \approx 1$ GeV, where the contribution of the isoscalar $^3D_3$ np partial wave is below the percent level.

Since interference must be discarded, we have to assume that a potential $d^*(2380)$ decay into the isoscalar $NN\pi$ channel adds incoherently to the conventional background. We observe, however, no indication of a corresponding enhancement in the energy dependence of the cross section. We can therefore only give an upper
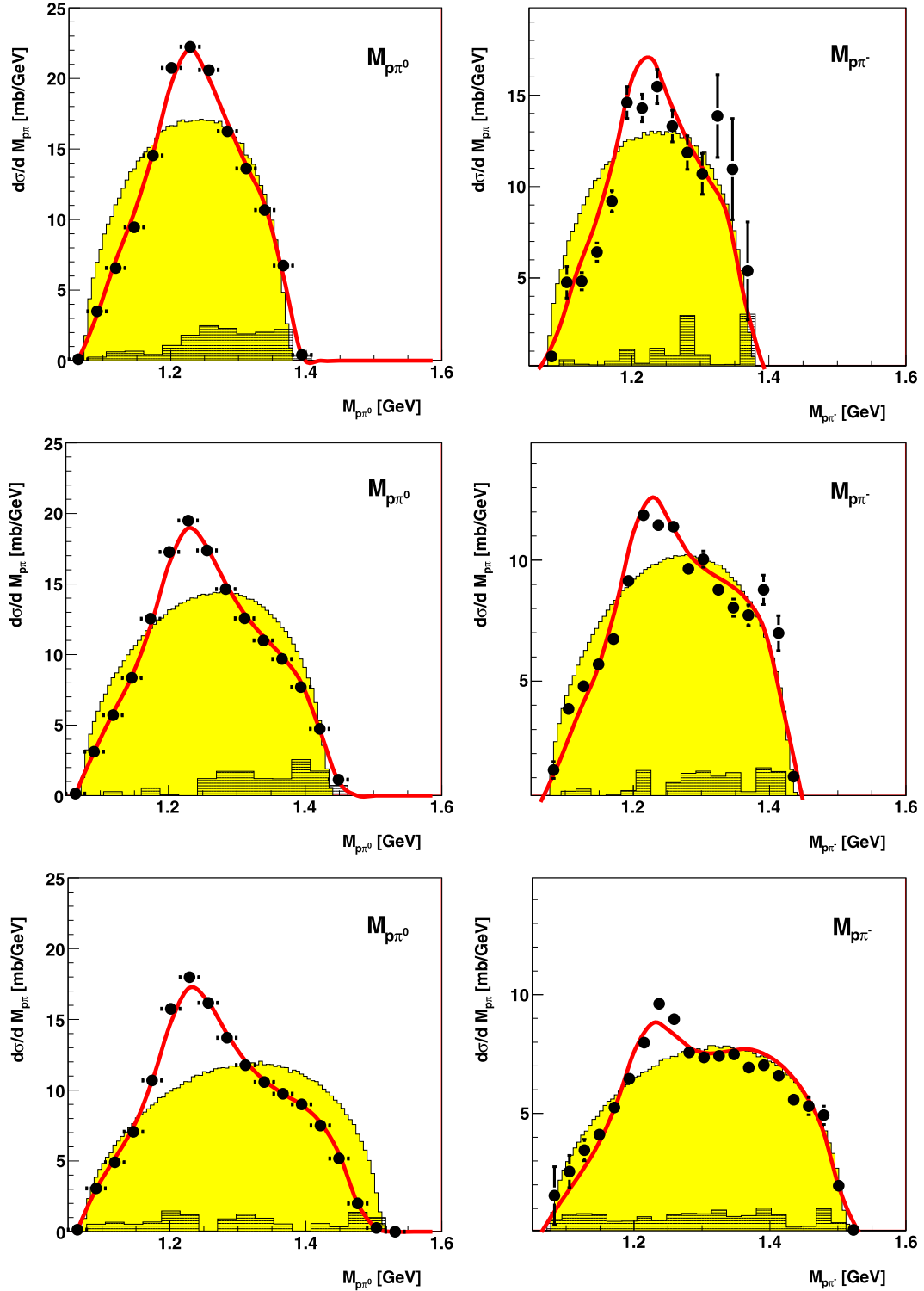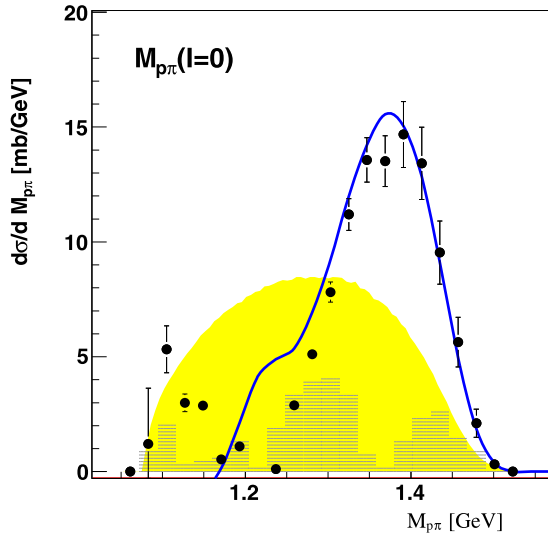
Fig. 5. (Color online.) The same as Fig. 3, but for the $M_{p\pi^0}$ (left) and $M_{p\pi^-}$ (right) spectra at $\sqrt{s} = 2.31$ GeV (top), 2.37 GeV (middle) and 2.45 GeV (bottom).

limit based on the statistical uncertainty of the data points in the $d^*(2380)$ resonance region.

The Roper resonance can be safely assumed to produce an isoscalar contribution, which has a very smooth energy dependence yielding a bump-like structure with a curvature representing the large width of the Roper. A Gaussian should therefore be a good approximation for the Roper contribution in the region of interest. Indeed, a corresponding fit gives already an excellent re-

production of our data. Inclusion of a Lorentzian representing a potential $d^*(2380)$ contribution gives an improvement only, if a tiny negative contribution of -35 ± 106 μb is allowed.

In order to get the right curvature at the low-energy side, we next included also the data of Dakhno et al. [5] in the fit, *i.e.*, the only ones, which consistently match to ours at the low-energy side. The inclusion of these data produces a slightly stronger curvature in the region of our data. The fit resulting in $m = 2310$ MeV $\approx$

Fig. 6. (Color online.) The same as Figs. 3 and 4, but for the isoscalar $p\pi$ invariant mass spectrum as obtained from the $M_{p\pi^0}$ and $M_{p\pi^-}$ distributions by use of eq. (1). The blue solid line represents the corresponding result from the t-channel calculations by use of eq. (1) normalized in area to the data.
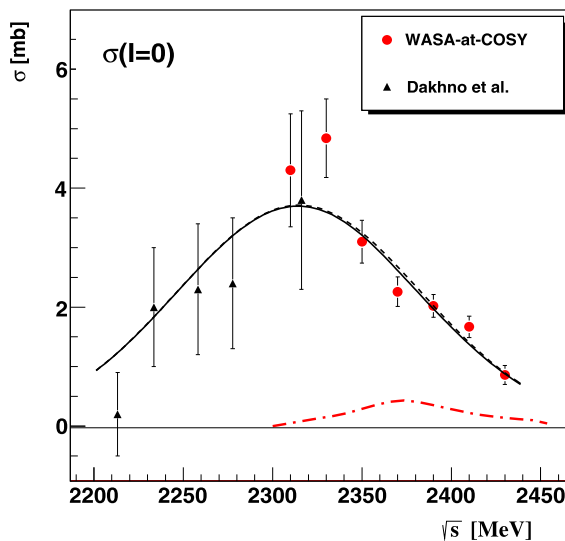
Fig. 7. (Color online.) The isoscalar single-pion production cross section in NN collisions in dependence of the total c.m. energy $\sqrt{s}$. Shown are the results of this work (circles) together with the results from Dakhno et al. [5] (triangles) at lower energies. The dash-dotted line illustrates a 10% $d^*(2380)$ resonance contribution. Solid and dashed lines show a fit to the data using a Gaussian with and without d^* contribution, respectively.

$m_{Roper} + m_N$ and $\Gamma = 170$ MeV $\approx \Gamma_{Roper}$, which is shown in Fig. 7 by the dashed line, yields an excellent description of both data sets. Inclusion of a potential $d^*(2380)$ contribution in the fit leads again to a negative resonance strength with a peak value of -65 ± 110 µb (solid line in Fig. 7). In both cases we find robust results, which are consistent with each other and consistent with an upper limit of 180 µb at the 90% confidence level. This value corresponds to an upper limit for the branching ratio of 9% for the $d^*(2380)$ decay into the $NN\pi$ channel.

This limit is much below the expectation, if $d^*(2380)$ would be dominantly a $N^*(1440)N$ configuration. As discussed in the introduction, for this case we expected a $d^*(2380)$ contribution of more than 1 mb. Hence this upper limit means that only less than 14% of the $d^*(2380)$ decay can proceed via a $N^*(1440)N$ configuration.

For the scenario, where the $d^*(2380)$ decay proceeds via the $D_{12}\pi$ configuration, our derived upper limit is not as stringent and restricts such a configuration only to less than 50%. Our result is compatible with a recent proposal to consider $d^*(2380)$ as a compact hexaquark configuration surrounded by a molecule-like $D_{12}\pi$ configuration [35]. It is, of course, also compatible with a pure hexaquark scenario, where the predicted $d^* \to NN\pi$ decay rate is as small as 1–3% [36].

4. Conclusions

The isoscalar single-pion production in NN collisions has been extracted from simultaneous measurements of the $pp \to pp\pi^0$ and $pn \to pp\pi^-$ reactions in the energy range $T_p = 0.95$–1.3 GeV ($\sqrt{s} = 2.3$–2.46 GeV). The obtained isoscalar cross sections in the region of 5 mb – the first ones in this energy range – fit well to earlier Gatchina results [5] at lower energies, but less to more recent ones [7,9].

The differential distributions of the $pp \to pp\pi^0$ and $pn \to pp\pi^-$ reactions are well described by t-channel meson exchange leading to excitation and decay of $\Delta(1232)$ and $N^*(1440)$. Application of eq. (1) to invariant-mass spectra provides an isoscalar $M_{p\pi}^{I=0}$ spectrum, where the $\Delta(1232)$ resonance is absent leaving thus the Roper resonance isolated.

The measured energy dependence of the isoscalar cross section gives no evidence for a decay of the dibaryon resonance $d^*(2380)$ into the isoscalar $NN\pi$ channel. The derived upper limit excludes the proposed $N^*(1440)N$ channel as a major intermediate decay configuration. It also restricts a possible $D_{12}\pi$ configuration to less than 50%, but is in full accordance with quark-model calculations predicting a compact hexaquark configuration for $d^*(2380)$. By these measurements the investigation of all possible hadronic decay channels of $d^*(2380)$ has been completed. What is left, is the study of its electromagnetic decays, which are expected to be smaller by another three to four orders of magnitude [37].

Acknowledgements

References

[1] M. Bashkanov, et al., Phys. Rev. Lett. 102 (2009) 052301.
[2] P. Adlarson, et al., Phys. Rev. Lett. 106 (2011) 242302.
[3] P. Adlarson, et al., Phys. Rev. Lett. 112 (2014) 202301.
[4] P. Adlarson, et al., Phys. Rev. C 90 (2014) 035204.
[5] L.G. Dakhno, et al., Phys. Lett. B 114 (1982) 409.
[6] J. Bystricky, et al., J. Phys. 48 (1987) 1901 and references therein.
[7] G. Rappenecker, et al., Nucl. Phys. A 590 (1995) 763 and references therein.
[8] W. Thomas, et al., Phys. Rev. D 24 (1981) 1736.
[9] V.V. Sarentsev, et al., Eur. Phys. J. A 21 (2004) 303.
[10] V.V. Sarentsev, et al., Eur. Phys. J. A 43 (2010) 11.
[11] M. Bashkanov, H. Clement, T. Skorodko, Eur. Phys. J. 51 (2015) 87 and references therein.
[12] M. Platonova, V. Kukulin, Phys. Rev. C 87 (2013) 025202.
[13] R.A. Arndt, J.S. Hyslop III, L.D. Roper, Phys. Rev. D 35 (1987) 128.
[14] R.L. Workman, W.J. Briscoe, I.I. Strakovsky, Phys. Rev. C 94 (2016) 065203.
[15] D.V. Bugg, Eur. Phys. J. A 50 (2014) 104.
[16] K.A. Olive, et al., PDG, Chin. Phys. C 38 (2014) 090001.
[17] Ch. Bargholtz, et al., Nucl. Instrum. Methods A 547 (2005) 294.
[18] H.H. Adam, et al., arXiv:nucl-ex/0411038, 2004.
[19] P. Adlarson, et al., Phys. Rev. C 90 (2014) 045207.
[20] F. Shimizu, et al., Nucl. Phys. A 386 (1982) 571.
[21] A.M. Eisner, et al., Phys. Rev. 138 (1965) B670.
[22] G. Agakishiev, et al., Eur. Phys. J. A 51 (2015) 137.
[23] A. Abdivaliev, et al., Dubna Preprint JINR D1-81-756, 1981.

[24] D.C. Brunt, M.J. Clayton, B.A. Westwood, Phys. Rev. 187 (1969) 1856.
[25] V. Flaminio, et al., CERN libraries, CERN-HERA 84-01, 1984.
[26] A.F. Dunaytsev, Y.D. Prokoshkin, Sov. Phys. JETP 9 (1959) 1179.
[27] S. Focardiet, et al., Nuovo Cimento 39 (1965) 405.
[28] B. Baldoni, et al., Nuovo Cimento 26 (1962) 1376.
[29] V.M. Guzhavin, et al., Sov. Phys. JETP 19 (1964) 847.
[30] R.J. Cence, et al., Phys. Rev. 131 (1963) 2713.
[31] D.V. Bugg, et al., Phys. Rev. 133 (1964) B1017.
[32] T. Skorodko, et al., Phys. Lett. B 679 (2009) 30.

[33] T. Skorodko, et al., Eur. Phys. J. A 35 (2008) 317.
[34] L. Alvarez-Ruso, E. Oset, E. Hernandez, Nucl. Phys. A 633 (1998) 519 and priv. comm.
[35] A. Gal, Phys. Lett. B 769 (2017) 436.
[36] Yubing Dong, Fei Huang, Pengnian Shen, Zongye Zhang, Phys. Lett. B 769 (2017) 223.
[37] H. Clement, Prog. Part. Nucl. Phys. 93 (2017) 195.